

# Reliability-based Sizing of Electric Propulsion System for Turboelectric Aircraft

Wang, Yebin; Lin, Chungwei; Fang, Huazhen; Takegami, Tomoki

TR2023-129 October 18, 2023

## Abstract

Aviation industry is moving towards more electric aircraft, where both non-propulsive and propulsive loads are electrified. While bringing in various benefits, electric propulsion system (EPS) introduces extra complexity and weight to aircraft, as well as raises the reliability concern. New design and analysis tools are required to size the EPS while meeting stringent reliability requirements. This paper investigates how to consolidate readability into the EPS sizing process and makes two-fold contributions. First, a probabilistic algorithm is proposed to assess the reliability of the EPS admitting a directed acyclic graph topology. The algorithm reduces the directed acyclic graph to a layered tree, which simplifies the calculation of joint probability of nodes in each layer. Second, we formulate the reliability-based EPS sizing as an integer nonlinear programming problem, where the reliability requirements are posed as constraints. Preliminary simulation validates the proposed method.

*IEEE Industrial Electronics Society (IECON) 2023*



# Reliability-based Sizing of Electric Propulsion System for Turboelectric Aircraft

Yebin Wang, Chung-Wei Lin, Huazhen Fang and Tomoki Takegami

**Abstract**—Aviation industry is moving towards more electric aircraft, where both non-propulsive and propulsive loads are electrified. While bringing in various benefits, electric propulsion system (EPS) introduces extra complexity and weight to aircraft, as well as raises the reliability concern. New design and analysis tools are required to size the EPS while meeting stringent reliability requirements. This paper investigates how to consolidate readability into the EPS sizing process and makes two-fold contributions. First, a probabilistic algorithm is proposed to assess the reliability of the EPS admitting a directed acyclic graph topology. The algorithm reduces the directed acyclic graph to a layered tree, which simplifies the calculation of joint probability of nodes in each layer. Second, we formulate the reliability-based EPS sizing as an integer nonlinear programming problem, where the reliability requirements are posed as constraints. Preliminary simulation validates the proposed method.

## I. INTRODUCTION

The strong correlation between greenhouse gas and climate change has made a compelling call for substantial cuts of greenhouse gas emissions in all sectors. Aviation industry, contributing roughly 2.1% of total human-induced CO<sub>2</sub> emissions, has been striving for energy efficient technologies, such as More Electric Aircraft (MEA) [1], to attenuate its environmental impact. MEA, electrifying both non-propulsive and propulsive loads, is envisioned to yield higher efficiency, controllability, reconfigurability, and ease of maintenance [2], [3]. Various Electrified Aircraft Propulsion systems have been proposed [4], [5], among which turboelectric propulsion concept has drawn intensive attention thanks to its excellent balance between technology readiness and potential fuel economy/environmental benefits. Turboelectric propulsion, facilitating distributed propulsion concepts such as Boundary Layer Ingestion, particularly prevails on long-haul air travel [6], [7].

Fig. 1 depicts the electric propulsion system (EPS) of an exemplary turboelectric propulsion system, where generator, AC/DC converter, cables, circuit breakers, DC/AC converter, motor, and fan (propulsor) are integrated to fulfill electric propulsion. At the source side, field-controlled synchronous generator or permanent magnet synchronous generator is driven by turbofan engine to produce electricity. At the load side, synchronous reluctance machine, induction machine, or permanent magnet synchronous motor drives the propulsor to yield thrust. In the middle, actively controlled or passive power

electronics convert electric power to accommodate system requirements on efficiency, weight, reliability, etc. Works [1], [6], [7] highlight key challenges in terms of EPS design, in order to strike a nice balance of eco-friendliness, economical benefits, airworthiness, and mission feasibility.

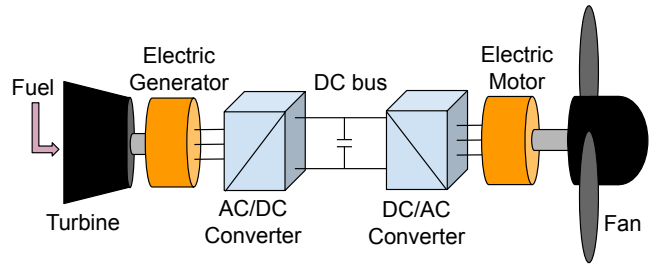


Fig. 1: A fully turboelectric propulsion system.

Reliability analysis has been one of the centerpieces for applications [8] such as power system [9] and aviation [10]. The latter weighs heavily on safety and size - all products have to meet certification [11] whilst fulfilling the mission. Reliability analysis has been applied to the entire lifecycle of aircraft: from component design [12], to system design [13], [14], to operation [15], and to schedule maintenance [16].

Aircraft reliability has been studied by using fault tree analysis, failure mode and effects analysis [17], [18], Bayesian network [15], [19], [20], Monte Carlo simulation [21], to name a few. Unlike full-fledged conventional propulsion system [22], EPS, as one of transformative technologies in aviation, remains at early stage and its reliability and sizing tools are in increasing demand. Recent work conduct reliability analysis for MEA [14], [20], [23]–[25]. For instance, work [20] evaluates the off-nominal performance and reliability of electric power architecture of a test distributed electric propulsion aircraft. Work [23] develops software to determine the reliability of a number of potential alternative design architectures.

The second critical requirement for aircraft is system weight, simply put, to determine the configuration and size of the EPS. Readers are referred to [26] about aircraft sizing. Work [14] incorporates the reliability analysis into the conceptual design of a fixed-wing Unmanned Aerial Vehicle. The design problem is solved by performing bi-level optimization: an outer-loop multi-objective optimization for the main design problem, and an inner-loop optimization for estimating the reliability index of a design solution. Similar treatment can be found in [13] to perform reliability-integrated wing design.

This work explores alternative approaches to assessing the reliability of an EPS and to integrating the reliability specifica-

Y. Wang and C.-W. Lin are with Mitsubishi Electric Research Laboratories, Cambridge, MA 02139, USA. Email: {yebinwang, clin}@merl.com.

H. Fang is with Department of Mechanical Engineering, University of Kansas, Lawrence, KS 66045, USA. Email: fang@ku.edu.

T. Takegami is with Advanced Technology R&D Center, Mitsubishi Electric Corporation, Amagasaki City, Japan. Email: Takegami.Tomoki@dy.MitsubishiElectric.co.jp.

tions into the EPS sizing during the aircraft conceptual design stage. The proposed reliability analysis method is analogous to [27]. The main difference is that we propose a systematic method to reduce a directed acyclic graph (DAG) into a layered tree structure, which is convenient for calculating the probability of failure rate of each node. We further perform reliability-based EPS sizing by solving an integer nonlinear programming problem (INLP) where the system failure rate enters the design equation as a constraint.

The remainder of this paper is organized as follows: Section II presents preliminaries and problem formulation, followed by the main reliability analysis results in Section III. Section IV reformulates, using an example, the sizing problem into an MINLP. The proposed reliability analysis and sizing methods are validated by simulation in Section V. Conclusions and future work are discussed in Section VI.

## II. PROBLEM FORMULATION

This section first presents concepts related to reliability analysis, introduces the EPS architecture, and finally formulates the reliability analysis-based EPS sizing problem.

### A. Preliminaries

Reliability is the ability of an item to perform as required in stated operating context and for a period of time [8]. This work assumes all components in the EPS are non-repairable, where the reliability can be measured by mean time to failure (MTTF) or failure rate. MTTF describes the expected time for a non-repairable system to fail and can be expressed as the expected value of  $f(t)$ :  $MTTF = \int_0^\infty t f(t) dt$ , where  $f(t)$  the density function of a random variable ‘time-to-failure’.

Failure rate, denoted by  $\lambda$ , is the frequency with which an engineered system or component fails, expressed in failures per unit of time. Assuming that the system has a time-to-failure density function  $f(t) = \lambda e^{-\lambda t}$  with a constant failure rate  $\lambda$ , the MTTF is obtained as  $MTTF = \frac{1}{\lambda}$ . In this work, the failure rate is adopted to quantify reliability.

### B. EPS Topology Modeling

We note that most of components (or units) in EPS allow bidirectional power flow. During normal operation, components facilitate the power flow from sources to loads. In the case that the motor runs in regenerative mode, power flows from loads to sources, e.g. batteries. However, the regenerative power is typically much less, and unlikely goes beyond the power ratings of units. Hence, the EPS sizing is concerned about the normal operation mode, where the EPS delivers power to produce thrust. Thus analysis here presumes that the EPS admits unidirectional power flow from sources to loads.

The topology of the unidirectional EPS is characterized by a directed acyclic graph (DAG)  $G(\mathcal{V}, \mathcal{E})$ , where  $\mathcal{V}$  and  $\mathcal{E}$  are the finite sets of nodes and directed edges, respectively. For a set  $\mathcal{V}$ ,  $|\mathcal{V}|$  denotes the number of its elements. Node  $q \in \mathcal{V}$  represents an electricity processing component and edge  $E(q_i, q_j)$  denotes the power flow from  $q_i$  to  $q_j$ . For node  $q$ , we denote the set of its parent nodes as  $\mathcal{V}_p(q) \triangleq \{q_{p1}, \dots, q_{pk_p}\}$

and the set of its child nodes as  $\mathcal{V}_c(q) \triangleq \{q_{c1}, \dots, q_{ck_c}\}$ , where  $k_p = |\mathcal{V}_p(q)|$  and  $k_c = |\mathcal{V}_c(q)|$ .

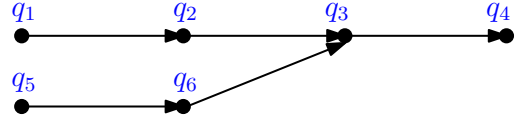


Fig. 2: The directed acyclic graph for a hybrid EPS where battery  $q_5$  operates in the discharging mode.

In the sequel, a DAG is referred to as ‘‘graph’’ for concise presentation. Without loss of generality, we assume that the DAG is connected. We denote the EPS as  $\Sigma_{EPS}$ . A graph can contain multiple root nodes and multiple target nodes. The former represent the power sources; and the latter represent the loads. Fig. 2 shows a graph comprising a node set  $\mathcal{V} : \{q_i, 1 \leq i \leq 6\}$  and an edge set  $\mathcal{E} : \{E(q_i, q_{i+1}) \text{ for } 1 \leq i \leq 3\} \cup \{E(q_5, q_6), E(q_6, q_3)\}$ . Specifically,  $q_1, q_2, q_3, q_4, q_5, q_6$  represent AC generator, AC/DC converter, DC/AC converter, motor, battery, and DC/DC converter, respectively.

We are interested in the EPS’s capability to deliver rated power to each load. Assume that load  $q_L$  fails to receive the rated power at the failure rate  $\lambda_{q_L}$ . We say EPS fails if any one of its load could not receive rated power. The EPS reliability is characterized by its failure rate  $\lambda_{\Sigma_{EPS}}$ , representing the highest failure rate of all loads.

**Remark II.1.** The DAG  $G(\mathcal{V}, \mathcal{E})$  characterizes the EPS of fully or partially turboelectric aircraft. For hybrid electric aircraft, one can readily use three directed acyclic graphs to represent the scenarios where battery operate at discharging, charging, and non-operative modes, respectively. During charging mode, there exist two power flows: 1)  $q_1 \rightarrow q_2 \rightarrow q_3 \rightarrow q_4$  and 2)  $q_1 \rightarrow q_2 \rightarrow q_6 \rightarrow q_5$ . Considering the fact that battery will take and store whatever surplus power from generators, the second power flow will not jeopardize the EPS’s capability of delivering propulsive power, and thus the second power flow can be eliminated.

We note that the number of generator, converters, and motor at each node can be more than 1: multiple units work in parallel. Let us denote the number of installed and used components as  $n_q^t$  and  $n_q^u$ , respectively.

### C. Problem Statement

This work deals with the reliability-based design of EPS, which involves three coupled pieces: topology (configuration) selection, reliability analysis, and EPS sizing. For simplicity, we ignore the topology selection problem and concentrate on the reliability analysis and EPS sizing.

Established methods of the propulsion system sizing during the conceptual design determines the rated powers of turbofan engine and the EPS on the basis of aircraft configuration/geometry and mission [28]. In this work, the rated power  $P_\Sigma^r$  of the EPS is given and the EPS sizing investigates the size and number of each component to ensure the successful delivery of the rated power. For the component at node  $q$ , its size

TABLE I: Node Properties

$\lambda_q$	failure rate
$\eta_q$	efficiency
$V_i$	information of input bus
$V_o$	information of output bus
$P_r$	rated (input) power
$i$	the layer number
$\mathcal{V}_p$	set of parent nodes
$key$	priority used in power allocation
$P_i$	input power
$P_o$	output power
$p_A$	probability of delivering rated output power

typically means the rated power  $P_q^r$ , which is closely related to how many components  $n_q^u$  are deployed during operation and how many  $n_q^t$  are installed. Given the topology  $\mathcal{G}$ , component technology  $\lambda_q$  and sizing  $n_q^t, n_q^u$ , one can quantify  $\lambda_{\Sigma_{EPS}}$ .

Define  $\Theta = [n_1^t, n_1^u, \dots, n_N^t, n_N^u]^T \in \mathbb{R}^{2N}$  where  $N$  indicates the number of nodes in  $\Sigma_{EPS}$ . The reliability-based sizing problem is stated as follows.

**Problem II.2.** Given an EPS with the topology graph  $G(\mathcal{V}, \mathcal{E})$ , determine the number of components at each node such that

- (i) each load node receives rated power with a failure rate below a threshold  $\underline{\lambda}$ ; and
- (ii) given a function  $J(\Theta) : \mathbb{R}^{2N} \rightarrow \mathbb{R}^+$  evaluating an EPS design, find  $\Theta^* = \arg \min_{\Theta} J(\Theta)$ .

Problem II.2 is divided into two steps: 1) assessing the reliability of a given EPS; and 2) searching for the best  $\Theta^*$  under reliability constraint.

### III. EPS RELIABILITY ANALYSIS

This section deals with the reliability analysis of an EPS with topology  $G$ . It establishes the probability that all loads successfully receive rated power from sources.

#### A. Modeling Node Probability

Node  $q$  has properties listed in Table I. As shown in Fig. 3, node  $q$  receives input power  $q.P_i$  from its parent nodes in  $\mathcal{V}_p(q)$ , processes the power at the efficiency  $\eta_q$  and the probability of failure  $\lambda_q$ , and outputs power  $q.P_o$  to its child nodes in  $\mathcal{V}_c(q)$ . Both  $q.P_i$  and  $q.P_o$  are random variables taking values over certain closed intervals in  $\{0\} \cup \mathbb{R}^+$ . Particularly,  $q.P_o$  depends on  $q.P_i$  as well as the failure rate  $\lambda_q$ . Define a binary random variable  $s_q$  take values over  $\{0, 1\}$ , with 1 meaning ‘‘function properly’’ and 0 otherwise. Variable  $s_q$  is governed by  $\lambda_q$ . Assuming that  $\lambda_q$  is independent from its input power, we have  $q.P_o = \eta_q \times s_q \times q.P_i$ , i.e.,

$$q.P_o = \begin{cases} \eta_q q.P_i, & \text{if } q \text{ works properly or } s_q = 1 \\ 0, & \text{otherwise.} \end{cases}$$

We compute the following two probabilities for node  $q$ :

- (i) the probability of random variable  $q.P_o$ , i.e.,  $\Pr(q.P_o)$
- (ii) the probability of the event  $A_q$  that node  $q$  outputs at least its rated power, i.e.,  $\Pr(q.P_o \geq q.P_r)$ .

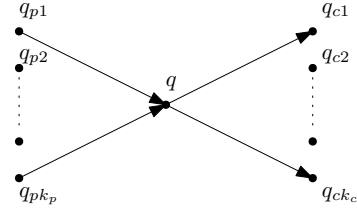


Fig. 3: Node probability

By applying Total Probability Theorem, probability  $\Pr(q.P_o)$  can be obtained as follows

$$\Pr(q.P_o) = \int_{\mathcal{V}_p(q).P_o} \Pr(q.P_o | \mathcal{V}_p(q).P_o) \Pr(\mathcal{V}_p(q).P_o), \quad (1)$$

where  $\mathcal{V}_p(q).P_o \triangleq \{q_{p1}.P_o, \dots, q_{pk_p}.P_o\}$ ,  $\Pr(q.P_o | \mathcal{V}_p(q).P_o)$  is conditional probability and  $\Pr(\mathcal{V}_p(q).P_o)$  is the joint probability of its parent nodes.

Because a parent node might serve multiple child nodes, the limited output power of the parent node has to be allocated among the child nodes. Hence,  $\Pr(q.P_o | \mathcal{V}_p(q).P_o)$  depends on how the power is allocated. We introduce scheduling decision  $S$  to represent how the power of parent nodes is allocated among child nodes. The conditional probability is reparameterized as  $\Pr(q.P_o | \mathcal{V}_p(q).P_o, S)$  to reflect its dependence on  $S$ . As long as  $S$  is deterministic and pre-defined,  $\Pr(q.P_o | \mathcal{V}_p(q).P_o, S)$  can be computed for the given power of parent nodes, and thus is treated as a priori. Combining with joint probability  $\Pr(\mathcal{V}_p(q).P_o)$ , one can readily calculate  $\Pr(q.P_o)$  according to formula (1). Given  $\Pr(q.P_o)$ , we can readily compute

$$\Pr(A_q) = \int_{q.P_o \in A_q} \Pr(q.P_o).$$

**Remark III.1.** Since the EPS sizing determines the rated capacity of each node, it is reasonable to say that node  $q$  always outputs rated power  $q.P_o$ , if working properly. That is:  $q.P_o$  takes values over the set  $\{0, q.P_r\}$ . By applying Total Probability Theorem,  $\Pr(q.P_o)$  is computed as follows

$$\Pr(q.P_o) = \sum_{\mathcal{V}_p(q).P_o} \{\Pr(q.P_o | \mathcal{V}_p(q).P_o, S) \Pr(\mathcal{V}_p(q).P_o)\}. \quad (2)$$

Because  $q.P_o$  is binary,  $\mathcal{V}_p(q).P_o$  contains  $2^{k_p}$  elements. Hence, joint probability  $\Pr(\mathcal{V}_p(q).P_o)$  is defined at  $2^{k_p}$  possible instances. One can calculate  $\Pr(q.P_o | \mathcal{V}_p(q).P_o, S)$  for each possible instance. If  $q_{k_i}.P_o$  is independent from the rest variables, (2) can be rewritten as (3).

#### B. Constructing Layered Tree

As shown in (1), the joint probability of parent nodes is necessary to calculate  $\Pr(q.p_o)$ . Since each node might have a distinct set of parent nodes  $\mathcal{V}_p(q)$ , calculating joint probability for the parent nodes of each node  $q$  becomes tedious and redundant. Next we show that the DAG  $G$  can be reduced to a layered tree, i.e., each node is assigned to a unique layer. All nodes in the  $i$ th layer is denoted by  $q_i$ . All nodes in the same layer have all nodes in the previous layer as the set of

$$\Pr(q.P_o) = \sum_{\mathcal{V}_p(q).P_o} \left\{ \Pr(q.P_o | \mathcal{V}_p(q).P_o, S) \times \Pr(q_{p1}.P_o, \dots, q_{pk_i-1}.P_o, q_{pk_i+1}.P_o, \dots, q_{pk_p}.P_o) \Pr(q_{pk_i}.P_o) \right\}. \quad (3)$$

parent nodes. Specifically, for nodes in the  $i$ th layer, the parent node set comprises all nodes of the  $i - 1$ th layer, i.e.,  $q_{i-1}$ . We only need to calculate the joint probability of the same set of parent nodes for all child nodes in the successive layer.

Given a DAG  $G(\mathcal{V}, \mathcal{E})$ , we propose Algorithm 1 to construct a layered tree  $\mathcal{T}$ . Let  $\mathcal{V}_s \triangleq \{q_{s1}, \dots, q_{s|\mathcal{V}_s|}\}$ ,  $\mathcal{V}_l \triangleq \{q_{l1}, \dots, q_{l|\mathcal{V}_l|}\}$  be the sets of source nodes and load nodes, respectively. Tree  $\mathcal{T}$  contains three priority queues  $Q$ ,  $Q_o$ ,  $Q_e$ , and  $n$  lists  $\mathcal{L}_i, 1 \leq i \leq n$  where  $n$  represents the number of layers. Here  $n$  is unknown in the beginning. List  $\mathcal{L}_i$  stores nodes in the  $i$ th layer. A closed list  $L_c$  contains the nodes which have been popped out of the priority queue. Note that all priority queues,  $Q, Q_o, Q_e$ , are ordered according to the  $g$ -value (or depth) of nodes. The pop operation returns and removes the node with the lowest  $g$ -value.

Queue  $Q_o$  stores junction nodes which connect to different source nodes and have different depth values. This is illustrated by Fig. 4 where  $q_3$  is a junction node, because two source nodes  $q_{s1}, q_{s2}$  can arrive. Particularly, the path from  $q_{s1}$  to  $q_3$  consists of two edges, and the node depth is 2; whereas the path from  $q_{s2}$  to  $q_3$  consists of one edge, and the node depth is 1. This inconsistency needs to be resolved.

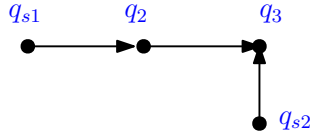


Fig. 4: Process junction node  $q_3$

Queue  $Q_e$  stores the pairs of nodes whose depths are inconsistent due to the presence of multiple paths between them, where the multiple paths are originated from one source node. As illustrated in Fig. 5, there exist two paths from  $q_{s1}$  to  $q_3$ : path #1 passes  $q_2$  and path #2 directly connects  $q_{s1}$ . Thus,  $q_3$  has depth values 2 and 1, corresponding to paths #1 and #2, respectively. We record  $q_3$  for further processing to determine its appropriate layer number.

For a DAG with multiple source nodes, starting from one source node and performing a modified breadth first algorithm (MBFA) on the DAG necessarily leaves other source nodes unvisited. Hence, we need to perform MBFA for all source nodes to construct  $\mathcal{T}$ , as shown in line 4 of Algorithm 1. Based on  $Q_o$  and  $Q_e$  in  $\mathcal{T}$ , PostProcessing resolves the inconsistency of depth values for all junction nodes and multi-path nodes.

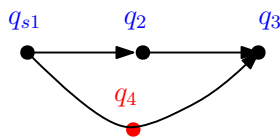


Fig. 5: Process multi-path node  $q_3$

#### Algorithm 1: Layered tree construction

```

1 input  $G(\mathcal{V}, \mathcal{E}), \mathcal{V}_s, \mathcal{V}_l$ ;
2  $\mathcal{T} \leftarrow \emptyset$ ;
3 for  $i = 1 : |\mathcal{V}_s|$  do
4    $\mathcal{T} \leftarrow \text{MBFA}(\mathcal{T}, G, q_{si})$ ;
5  $\mathcal{T} \leftarrow \text{PostProcessing}(\mathcal{T})$ ;
6 return  $\mathcal{T}$ ;

```

MBFA is given in Algorithm 2. When invoked for the first time with  $q_{s1}$ , MBFA constructs a layered tree  $\mathcal{T}_1$  where all load nodes are visited and constitute all the leaves. Running MBFA with source node  $q_{si}$  will visit two types of nodes and update their  $g$ -value (Lines 13-16):

- (i) nodes serviced by  $q_{si}$  but have not been expanded; and
- (ii) nodes giving a larger  $g$ -value if following the path from  $q_{si}$  (more distant from  $q_{si}$  than all previously visited source nodes  $q_{s1}, \dots, q_{si-1}$ ).

FetchChild( $q$ ) returns the set of child nodes for node  $q$ . If a child node  $q_{ci}$  has been visited and belongs to the closed list  $L_c$ , which implies node  $q_{ci}$  is a multi-path node, then we push node  $q_{ci}$  into  $Q_o$ . In fact, any node having more than one parent node will appear in  $Q_o$ .

#### Algorithm 2: MBFA

```

1 input  $\mathcal{T}, G(\mathcal{V}, \mathcal{E}), q_{si}$ ;
2  $Q \leftarrow \emptyset$ ;  $Q_o \leftarrow \emptyset$ ;  $Q_e \leftarrow \emptyset$ ;  $L_c \leftarrow \emptyset, q_{si}.g = 0$ ;
3  $Q.\text{push}(q_{si})$ ;
4 while  $Q$  is not empty do
5    $q \leftarrow Q.\text{pop}$ ;  $L_c.\text{push}(q)$ ;
6    $\mathcal{V}_c(q) \leftarrow \text{FetchChild}(q)$ ;
7   // breadth first forward search;
8   for  $i = 1 : |\mathcal{V}_c(q)|$  do
9     // add new junction nodes ;
10    if  $q_{ci} \in \mathcal{T}.L_c$  and  $q \notin \mathcal{T}.L_c$  then
11       $Q_o.\text{push}(q_{ci})$ ;
12    // add multi-path nodes rooted at  $q_{si}$ ;
13    if  $q_{ci} \in L_c$  then
14       $Q_e.\text{push}(q_{ci})$ ;
15    // record the max depth value of node;
16    if not  $q_{ci}.\text{visited}$  or  $q_{ci}.g < q.g + 1$  then
17       $q_{ci}.g = q.g + 1$ ;
18       $q_{ci}.\text{visited} = \text{true}$ ;
19       $Q.\text{push}(q_{ci})$ ;
20  $\mathcal{T}.Q_o \leftarrow Q_o \cup \mathcal{T}.Q_o$ ;
21  $\mathcal{T}.Q_e \leftarrow Q_e \cup \mathcal{T}.Q_e$ ;
22  $\mathcal{T}.L_c \leftarrow L_c \cup \mathcal{T}.L_c$ ;
23 return  $\mathcal{T}$ ;

```

**Proposition III.2.** After invoking MBFA for all source nodes, any node in  $G$  has been visited and assigned a  $g$ -value representing its depth from a certain source node. The  $g$ -value

of any node in  $Q_o$  and beyond (toward load nodes) represents the number of steps of the longest path from source nodes to the node.

*Proof.* Proof is omitted due to space limitation.  $\square$

The MBFA does not address the two cases depicted in Figs. 4-5. Particularly, for Fig. 4 scenario,  $q_3.g = 2$  whereas  $q_{s2}.g = 1$ . For Fig. 5, after MBFA, we have  $q_{s1}.g = 1$  by following the path  $q_{s1} \rightarrow q_1 \rightarrow q_2$  or  $q_{s1}.g = 1$ . However, the  $g$ -value should be 1 if following the path  $q_{s1} \rightarrow q_3$ . PostProcessing resolves these inconsistencies. In Lines 4-9 of Algorithm 3, we visit multi-path nodes one by one, and for each node, insert  $(q.g - q_{pi}.g - 1)$  number of virtual nodes between  $q$  and  $q_{pi}$ . In Fig. 5, we embed node  $q_4$  into the path  $q_{s1} \rightarrow q_3$  so that  $q_{s1}.g$  is well-defined. Note that this operation does not alter  $g$ -values of all existing nodes. In Lines 11-20, we conduct a backward breadth first search: given a node  $q \in Q_o$ , we update the  $g$ -values of nodes whose  $g$ -values are inconsistent with their child nodes.

**Algorithm 3: PostProcessing**

```

1 input  $\mathcal{T}$ ;
2  $Q_o \leftarrow \mathcal{T}.Q_o$ ;  $Q_e \leftarrow \mathcal{T}.Q_e$ ;
3 // process multi-path nodes;
4 while  $Q_e$  is not empty do
5    $q \leftarrow Q_e.pop$ ;
6    $\mathcal{V}_p(q) \leftarrow \text{FetchParent}(q)$ ;
7   for  $i = 1 : |\mathcal{V}_p(q)|$  do
8     if  $q_{pi}.g \neq q.g - 1$  then
9        $\mathcal{T} \leftarrow \text{AddVirtualNodes}(\mathcal{T}, q, q_{pi})$ ;
10 // process junction nodes;
11 while  $Q_o$  is not empty do
12    $q \leftarrow Q_o.pop$ ;
13    $Q \leftarrow \emptyset$ ;  $Q.push(q)$ ;
14   while  $Q$  is not empty do
15      $q \leftarrow Q.pop$ ;
16      $\mathcal{V}_p(q) \leftarrow \text{FetchParent}(q)$ ;
17     for  $i = 1 : |\mathcal{V}_p(q)|$  do
18       if  $q_{pi}.g < q.g - 1$  then
19          $q_{pi}.g = q.g - 1$ ;
20          $Q.push(q_{pi})$ ;
21 return  $\mathcal{T}$ ;

```

By applying Algorithms 1 - 3 to an EPS topology in DAG, one can obtain a layered tree structure.

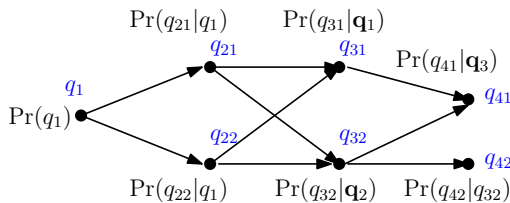


Fig. 6: An example of the layered tree structure

### C. Calculating Node Probability

The discussion below is based on the layered tree structure which is exemplified by Fig. 6. The EPS admits a layered tree with  $n$  layers, where the  $i$ th layer contains  $k_i$  nodes, and  $q_{i,j}$  denotes the  $j$ th node in the  $i$ th layer. All nodes at the  $i$ th layer have the same parents: all nodes at the  $i - 1$ th layers.

Given the  $n$  layered tree, probabilities of all source nodes, specification of all nodes, and failure rates of all nodes, one can calculate the joint probability of all nodes in each layer iteratively in a forward propagation manner. That is: at the  $i$ th layer for  $i = 2, \dots, n$ , we calculate  $\Pr(\mathbf{q}_i)$  of the  $i$ th layer, based on the joint probability distribution of all nodes at the previous layer and conditional probability  $\Pr(\mathbf{q}_i | \mathbf{q}_{i-1}, S)$ . We repeat the process until  $i = n$ .

Generally, the sum of the rated output power of nodes  $\mathbf{q}_i$  has to be greater than the rated input power of nodes  $\mathbf{q}_{i+1}$ . This means if all nodes operate well, then the power balance always holds. This is not true if some nodes in  $\mathbf{q}_i$  fail. In such cases, the output power of  $\mathbf{q}_i$  is allocated to  $\mathbf{q}_{i+1}$ , preferably in a deterministic manner. How to assign the power to child nodes is a scheduling problem. Different scheduling problems can be formulated to optimize individual objectives, and thus render distinct solutions, referred to as schedules. Solving scheduling problems through optimization could be time-consuming. Instead, certain heuristic rules can be defined to choose which child node gets the power first. From system safety perspective, a simple but realistic rule is: the parent nodes always try to meet the power demand of the most critical child nodes at first. Another rule, from system efficiency perspective, is: the parent nodes prioritize power toward most efficient child nodes.

Given  $\mathbf{q}_i$  and scheduling decision  $S_i$ , one can construct conditional probability  $\Pr(\mathbf{q}_{i+1} | \mathbf{q}_i)$ . Considering that  $q_{ij}$  is a binary variable, one writes  $\Pr(\mathbf{q}_{i+1} | \mathbf{q}_i)$  as a transition matrix  $M_{i+1,i}(S_i)$ , which is a  $2^{k_{i+1}} \times 2^{k_i}$ -dimensional matrix. Then formula (2) admits a vector form:  $\text{vec}(\Pr(\mathbf{q}_{i+1})) = M_{i+1,i}(S_i)\text{vec}(\Pr(\mathbf{q}_i))$ , where  $\text{vec}(\Pr(\mathbf{q}_{i+1}))$  and  $\text{vec}(\Pr(\mathbf{q}_i))$  are vectors in appropriate dimensions. Once we have the joint probability  $\Pr(\mathbf{q}_i)$ , the probability of  $\Pr(A_q)$  for node  $q$  can be readily calculated.

**Example III.1.** For illustration purpose, assume all nodes have efficiency 1. Let node  $q_{11}.p_o = q_{21}.p_i = q_{22}.p_i = 1$ , and node  $q_{12}.p_o = q_{21}.p_i + q_{22}.p_i = 2$ . The non-zero conditional probability  $\Pr(\mathbf{q}_2 | \mathbf{q}_1)$  is given by Table II. Here we prioritize the power supply toward  $q_{21}$  over  $q_{22}$ .  $\blacksquare$

## IV. RELIABILITY-BASED SYSTEM SIZING AND CONFIGURATION TRADE STUDY

In this section, Problem II.2 is formulated as an INLP. For illustration purpose, let us consider the EPS shown in Fig. 7, where generator, AC/DC converter, DC/AC converter, and motor are connected in series. The EPS topology has been put into the layered tree structure. All generators and converters are assumed fully connected: any generator can serve any converter if needed. Similarly, inverters and motors

TABLE II: Conditional probability

$(q_{11}.Po, q_{12}.Po)$	$(q_{21}.Pi, q_{22}.Pi) = (0, 0)$	$(q_{21}.Pi, q_{22}.Pi) = (1, 0)$	$(q_{21}.Pi, q_{22}.Pi) = (0, 1)$	$(q_{21}.Pi, q_{22}.Pi) = (1, 1)$
(0, 0)	1	0	0	0
(1, 0)	0	1	0	0
(0, 2)	0	0	0	1
(1, 2)	0	0	0	1

are fully connected. Node  $q$  might contain a total number of  $n_q^t$  units installed, where  $n_q^u$  is the number of units in use to deliver rated power, and  $n_q^r = n_q^t - n_q^u$  is the number of backup units. We further assume that any unit failure can be mitigated instantaneously by deploying a backup unit without the interruption of service. Problem II.2 is reduced to determine parameters in Table III.

TABLE III: System design parameters

Notation	Description	Note
$n_1^t, n_1^u$	total and used number of generators	integer
$n_2^t, n_2^u$	total and used number of AC/DC converters	integer
$n_3^t, n_3^u$	total and used number of DC cables	integer
$n_4^t, n_4^u$	total and used number of DC/AC converters	integer
$n_5^t, n_5^u$	total and used number of motors	integer
$n_6^t, n_6^u$	total and used number of propulsors	integer

To simplify presentation, we introduce a set of node indices  $\mathcal{I} : \{1, \dots, 6\}$ . System power is related to decision variables  $n_q^t, n_q^u$ . We have for the  $k$ th node,

$$n_k^u \rho_k^p m_k \geq S_p, \quad \forall k \in \mathcal{I},$$

where  $m_k$  and  $\rho_k^p$  are the weight and the specific power density, respectively; and  $S_p$  is the power supplied to load nodes. For a unit, denote the unit power  $P_k$  for  $k \in \mathcal{I}$ .

Heat balance arises from the fact that power losses of all units turn into heat and have to be dissipated properly. For the  $k$ th unit, with the rated power  $P_k^r$  and power efficiency  $\eta_k$ , the power losses is  $P_k^r(1 - \eta_k)$ . In many cases, the heat has to be removed by using coolant, which incurs additional system weight and power consumption.

Optimization-based system design problem formulation boils down to turn system physics and customer requirements into constraints and objective function. We have constraints

$$\begin{aligned}
 & -n_k^u P_k^r \leq -S_p, \text{ power balance for } k \in \mathcal{I} \\
 & \lambda_{\Sigma_{\text{EPS}}} \leq S_f = 10^{-9}, \text{ reliability requirement} \\
 & \sum_{k \in \mathcal{I}} n_k^t \leq S_N = 100, \text{ complexity requirement} \\
 & n_k^t, n_k^u \text{ are positive integers, } \forall k \in \mathcal{I} \\
 & 1 \leq n_k^u \leq n_k^t.
 \end{aligned} \quad (4)$$

The objective function is the system weight given by  $J = S_{w1} + S_{wc}$  with

$$\begin{aligned}
 S_{w1} &= \sum_{k \in \mathcal{I}} n_k^t m_k, \text{ component weight} \\
 S_{wc} &= \sum_{k \in \mathcal{I}} c_k n_k^u P_k^r \eta_k, \text{ coolant weight,}
 \end{aligned}$$

where  $c_k$  is the coefficient from power loss to coolant weight for the  $k$  component. Finally we formulate the EPS sizing as the following MINLP problem:

$$\min_{\{n_k^t, n_k^u, k \in \mathcal{I}\}} J \quad \text{subject to (4)}. \quad (5a)$$

**Remark IV.1.** Given the SPD of  $k$ th unit and the number of units to be used, the power constraint can be satisfied as long as the component weights more than  $S_p / (n_k^u \rho_k^p)$ . With this, the power constraint can be removed, while the component weight admits the following formula  $S_{w1} = \sum_{k \in \mathcal{I}} \frac{n_k^t S_p}{n_k^u \rho_k^p}$ . This makes the cost function nonlinear in  $n_k^u$ .

## V. SIMULATION

We conduct reliability assessment for a system represented by Fig. 7. Assume that all units in a particular layer have the same specifications. With the data shown in Table IV, we calculate the probability that each node receives rated power as shown in Fig. 8. The calculation shows that the system's failure rate does not meet the requirement.

TABLE IV: Component specifications

Notation	Rate power	Failure rate	Power density
$q_{11}, q_{12}, q_{13}$	1MW	$10^{-6}$	9kW/kg
$q_{21}$	2MW	$5 \times 10^{-6}$	20kW/kg
$q_{31}$	2MW	$10^{-10}$	10kW/kg
$q_{41}, q_{42}, q_{43}$	1MW	$5 \times 10^{-6}$	20kW/kg
$q_{51}, q_{52}, q_{53}$	1MW	$1 \times 10^{-6}$	10kW/kg
$q_6$	2MW	$10^{-10}$	10kW/kg

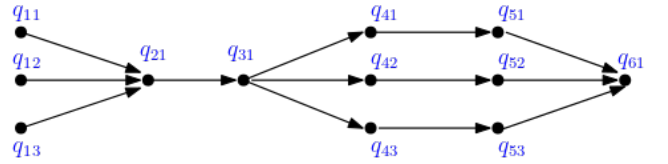


Fig. 7: EPS example in layered tree structure

Given the topology of EPS, we can further conduct sizing: determine the number of units to be installed at each node. For the EPS as shown in Fig. 7, reliability analysis shows that installing 1 unit in the second layer does not provide required reliability. In order to determine how many units are needed at each layer, we first simplify the topology into a string, by collapsing all units in a layer into one node. Hence, Problem II.2 is solved to determine the number of units. Let the upper and lower bounds of units can be installed for layer  $\{1, \dots, 6\}$  be 5, 8, 3, 8, 5, 5, respectively. We formulate the INLP to minimize the system weight using CasADi [29], and use Bonmin@ to solve for the solution given by

$$n_1^t = 5, n_1^u = 4, w_1^t = 277.78 \text{ kg}$$

$$\begin{aligned}
n_2^t &= 8, n_2^u = 7, w_2^t = 114.29\text{kg} \\
n_3^t &= 3, n_3^u = 2, w_3^t = 300\text{kg} \\
n_4^t &= 8, n_4^u = 7, w_4^t = 114.29\text{kg} \\
n_5^t &= 5, n_5^u = 4, w_5^t = 250\text{kg} \\
n_6^t &= 5, n_6^u = 4, w_6^t = 250\text{kg}.
\end{aligned}$$

The system has a failure rate  $10^{-9}$  and weight 1306.3kg.

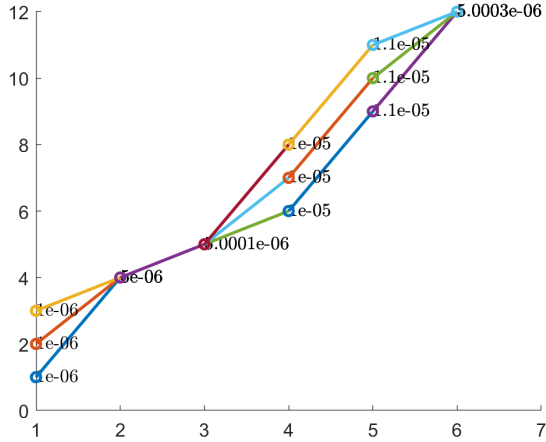


Fig. 8: Reliability assessment: node failure probability.

## VI. CONCLUSIONS AND FUTURE WORK

This paper presented a probabilistic algorithm to assess the EPS reliability. Based on the reliability assessment, the EPS sizing problem was formulated as an INLP which can be solved by using open-source optimization software. Simulation validated the proposed methods. We note that both the original INLP and its relaxation are challenging to solve. The former is mainly because of its combinatory nature, whereas the latter is due to lack of accurate gradient approximation. Future extensions are 1) developing methods to solve the relaxation problem; and 2) integrating reliability estimate, sizing, and topology selection in a systematic manner.

## REFERENCES

- [1] B. Sarlioglu and C. T. Morris, "More electric aircraft: Review, challenges, and opportunities for commercial transport aircraft," *IEEE Transactions on Transportation Electrification*, vol. 1, no. 1, pp. 54–64, 2015.
- [2] M. Sinnott, "B787 No-Bleed systems: Saving fuel and enhancing operational efficiencies," *Aero Quarterly*, vol. 18, pp. 6–11, 2007.
- [3] S. Bozhko, C. I. Hill, and T. Yang, "More-electric aircraft: Systems and modeling," *Wiley encyclopedia of electrical and electronics engineering*, pp. 1–31, 2018.
- [4] D. K. Hall, A. C. Huang, A. Uranga, E. M. Greitzer, M. Drela, and S. Sato, "Boundary layer ingestion propulsion benefit for transport aircraft," *Journal of Propulsion and Power*, vol. 33, no. 5, pp. 1118–1129, 2017.
- [5] J. L. Kratz and G. L. Thomas, "Dynamic analysis of the STARC-ABL propulsion system," in *AIAA Propulsion and Energy 2019 Forum*, 2019, p. 4182.
- [6] A. S. Gohardani, G. Doulergeris, and R. Singh, "Challenges of future aircraft propulsion: A review of distributed propulsion technology and its potential application for the all electric commercial aircraft," *Progress in Aerospace Sciences*, vol. 47, no. 5, pp. 369–391, 2011.

- [7] J. Benzaquen, J. He, and B. Mirafzal, "Toward more electric powertrains in aircraft: Technical challenges and advancements," *CES Transactions on Electrical Machines and Systems*, vol. 5, no. 3, pp. 177–193, 2021.
- [8] M. Rausand and A. Hoyland, *System reliability theory: models, statistical methods, and applications*. John Wiley & Sons, 2003, vol. 396.
- [9] D. C. Yu, T. C. Nguyen, and P. Haddawy, "Bayesian network model for reliability assessment of power systems," *IEEE Transactions on Power Systems*, vol. 14, no. 2, pp. 426–432, 1999.
- [10] D. Pettit and A. Turnbull, "General aviation aircraft reliability study," Tech. Rep., 2001.
- [11] M. S. Saglimbene, "Reliability analysis techniques: How they relate to aircraft certification," in *2009 Annual Reliability and Maintainability Symposium*, 2009, pp. 218–222.
- [12] R. Burgos, G. Chen, F. Wang, D. Boroyevich, W. G. Odendaal, and J. D. V. Wyk, "Reliability-oriented design of three-phase power converters for aircraft applications," *IEEE Transactions on Aerospace and Electronic Systems*, vol. 48, no. 2, pp. 1249–1263, 2012.
- [13] X. Yu and X. Du, "Reliability-based multidisciplinary optimization for aircraft wing design," *Structures and Infrastructure Engineering*, vol. 2, no. 3-4, pp. 277–289, 2006.
- [14] P. Champasak, N. Panagant, N. Pholdee, G. A. Vio, S. Bureerat, B. S. Yildiz, and A. R. Yildiz, "Aircraft conceptual design using metaheuristic-based reliability optimisation," *Aerospace Science and Technology*, vol. 129, p. 107803, 2022.
- [15] W.-H. Pan, Y.-W. Feng, C. Lu, and X.-F. Xue, "Adoption of a bayesian network for the operational reliability analysis of aircraft systems," in *IOP Conference Series: Materials Science and Engineering*, vol. 1043, no. 2, 2021, p. 022055.
- [16] J.-N. Yang and W. J. Trapp, "Inspection frequency optimization for aircraft structures based on reliability analysis," *Journal of aircraft*, vol. 12, no. 5, pp. 494–496, 1975.
- [17] J. Li and H. Xu, "Reliability analysis of aircraft equipment based on FMECA method," *Physics Procedia*, vol. 25, pp. 1816–1822, 2012.
- [18] W. Jiang, C. Xie, B. Wei, and D. Zhou, "A modified method for risk evaluation in failure modes and effects analysis of aircraft turbine rotor blades," *Advances in Mechanical Engineering*, vol. 8, no. 4, p. 1687814016644579, 2016.
- [19] Y. C. Tong, "Literature review on aircraft structural risk and reliability analysis," 2001.
- [20] M. V. Bendarkar, D. Sarojini, and D. N. Mavris, "Off-nominal performance and reliability of novel aircraft concepts during early design," *Journal of Aircraft*, vol. 59, no. 2, pp. 400–414, 2022.
- [21] K. Kurien, G. Sekhon, and O. Chawla, "Analysis of aircraft reliability using Monte Carlo simulation," *International Journal of Quality & Reliability Management*, vol. 10, no. 2, 1993.
- [22] K.-H. Chang, C.-H. Cheng, and Y.-C. Chang, "Reliability assessment of an aircraft propulsion system using IFS and OWA tree," *Engineering Optimization*, vol. 40, no. 10, pp. 907–921, 2008.
- [23] R. D. Telford, S. J. Galloway, and G. M. Burt, "Evaluating the reliability & availability of more-electric aircraft power systems," in *47th International Universities Power Engineering Conference (UPEC)*, 2012, pp. 1–6.
- [24] J. Harikumar, G. Buticchi, M. Galea, A. Costabeber, and P. Wheeler, "Reliability analysis of aircraft starter generator drive converter," in *15th Brazilian Power Electronics Conference and 5th IEEE Southern Power Electronics Conference (COBEP/SPEC)*, 2019, pp. 1–6.
- [25] Y. Zhang, J. Xia, X. Zhang, Z. Chen, B. Li, Q. Luo, and Y. He, "Modeling and prediction of the reliability analysis of an 18-pulse rectifier power supply for aircraft based applications," *IEEE Access*, vol. 8, pp. 47 063–47 071, 2020.
- [26] D. P. Raymer, *Aircraft Design: A Conceptual Approach*. American Institute of Aeronautics and Astronautics, Inc., 2018.
- [27] J. G. Torres-Toledano and L. E. Sucar, "Bayesian networks for reliability analysis of complex systems," in *Progress in Artificial Intelligence—6th Ibero-American Conference on AI*, 1998, pp. 195–206.
- [28] J. Welstead and J. L. Felder, "Conceptual design of a single-aisle turbo-electric commercial transport with fuselage boundary layer ingestion," in *54th AIAA aerospace sciences meeting*, 2016, p. 1027.
- [29] J. A. E. Andersson, J. Gillis, G. Horn, J. B. Rawlings, and M. Diehl, "CasADi – A software framework for nonlinear optimization and optimal control," *Mathematical Programming Computation*, vol. 11, pp. 1–36, 2019.